Review Article

Synthesis of Titanium Oxide (TiO_2) Nanoparticle and Its Application for Photocatalytic Degradation of Ortho-Nitroaniline Orange

Shamsuddeen Musa[1,*], Auwal Mahmoud Adamu[1], Dahiru Adamu Ajiya[1], Samuel Adebayo Adeyanju[2]

[1]*Department of Chemistry, Faculty of Science, Abubakar Tafawa Balewa University, Bauchi, Nigeria*
[2]*Federal University of Technology, Akure, Ondo State, Nigeria*

Citation S. Musa, A.M. Adamu, D.A. Ajiya, S.A Adeyanju. Synthesis of Titanium Oxide (TiO_2) Nanoparticle and Its Application for Photocatalytic Degradation of Ortho-Nitroaniline Orange. *J. Eng. Ind. Res.* **2026**, 7(3):137-143.

https://doi.org/10.48309/jeires.2026.542860.1314

Article info:
Submitted: 2025-09-15
Revised: 2025-12-08
Accepted: 2025-12-28
ID: JEIRES-2509-1314

Keywords:
TiO_2 nanoparticles, PANI/TiO_2 nanocomposite, Photocatalysis, Dye degradation.

ABSTRACT

Wastewater that is polluted with synthetic dyes presents a major environmental problem and treatment by conventional methods usually does not lead to full elimination of the dyes. The industry desperately looks for eco-friendly solutions that involve the use of photocatalysts that can efficiently remove toxic organic dyes from water. In recent years, polymer nanocomposites have become a significant focus in both academic and industrial fields. Nanoparticles are materials that are smaller than 100 nanometers in size. Adding a small amount of nanoparticles to polymers can give the composite materials new properties. This research describes how to make titanium oxide (TiO_2) nanoparticles using the sol-gel method. The nanoparticles were characterized using FTIR, X-ray diffraction (XRD), and UV-Visible spectroscopy. From the UV-Visible results and using a Tauc plot, the band gap energy of polyaniline/TiO_2 nanoparticles was calculated. The X-ray diffraction data also showed the size of the crystalline particles. The UV radiation caused a total of 98% ortho nitroaniline orange dye degradation under the action of the Mg^{2+}-doped PANI/TiO_2 nanocomposite, which had a 3.0 eV band gap and 38.7 nm crystalline size. The isotherm and kinetics studies verified the adsorption to be effective and the photocatalytic activity to be rapid. This indicates that the composite can be used to develop an eco-friendly dye remediation process for water treatment. Future research needs to address the photocatalytic activity of Mg^{2+}-doped TiO_2 nanocomposites associated with visible light and real industrial wastewater situations.

Introduction

In recent years, nanotechnology has become a promising tool for scientific innovations. Generally, composite materials are solid substances made by combining two or more simple materials, creating a continuous phase and a dispersed phase [1]. Nanoscience and technology have been widely explored. Conducting polymers have been thoroughly studied over the past decade and are used in various technological applications such as electrochromic devices, batteries, biosensors, gas separation membranes, enzyme immobilization matrices, and protection against metal corrosion [2]. They have drawn much attention in the area of active materials, especially for use in devices like organic light emitting diodes (OLEDs), field-effect transistors

*Corresponding Author: Shamsuddeen Musa (shamsuddeenmusa558@gmail.com)

(OFETs), and solar cells [3]. One of the most promising and widely studied metal oxides is TiO_2 because of its special physical, chemical, optical, electrical, and photoelectric conversion efficiency [4-6]. Due to their remarkable thermal, optical, electrical, and magnetic properties, metal oxide nanoparticles are among the most widely applied materials, and among these, TiO_2 nanoparticles stand out [7-10]. The only natural form of titanium oxide is rutile. Under normal conditions, TiO_2 is an odorless and snow-white powder that is hydrophobic in nature. Furthermore, it is regarded as a very stable substance that also serves as an excellent opacifier [11-13]. Its key properties include minimum cost, high oxidizing strength, great chemical stability, high refractive index, and the presence of oxygen-containing functional groups in its lattice [14]. TiO_2 NPs find wide application as a semiconductor material mainly because of these characteristics. In 2011, global TiO_2 production reached over 10,000 tons annually for the first time [15]. They can also be employed for the destruction of bacteria, viruses, and even tumor cells among microorganisms. UV light resistant oxides, toothpastes, papers, food colorants, paints, and plastics, as well as inks, all have them in their composition. Among the solar collectors, TiO_2 NPs are the most efficient, particularly because they can absorb 3 to 4 percent of the sun's energy. Consequently, they are recognized as excellent photocatalysts not only for hydrogen production, but also for the decomposition of hazardous organic compounds in water. The surface properties and topologies of TiO_2 NPs are unique. TiO_2 is a metal oxide that is light in color, a solid inert, and a compound. Three different polymorphs exist in TiO_2 NPs: anatase, rutile, and brookite. Anatase and rutile polymorphs are alike in many respects such as their luster, hardness, densities, and they also share similar type of symmetry (tetragonal) [16-20]. TiO_2 it is common in nature, stays stable under high electric fields, has a wide energy gap, a large surface area, is not harmful, has a good dielectric constant, is easy to make, and is friendly to the environment [21]. Many studies have looked into adding transition metals, rare earth elements, and noble metal ions to TiO_2 [22-25]. However, adding Mg^{2+} ions, which are from an alkaline earth metal to the TiO_2/POT composite, has not been studied before. So, in this study, the Mg^{2+} ion doped TiO_2 composite was made and examined using the in-situ oxidative polymerization method [25-27].

Materials and Methods

A complete assortment of apparatus and chemical reagents was no doubt necessary to carry out the synthesis and characterization of Mg^{2+}-doped polyaniline/titanium oxide (PANI/TiO_2) nanocomposites very successfully. A Rigaku MiniFlex 600 X-ray diffractometer together with Dynamic Light Scattering (DLS) through CILAS NanoDS was applied for precise structural and morphological analysis to establish crystallinity and particle size, while the former was used for particle size distribution measurements. A PerkinElmer Frontier Fourier-transform infrared spectrometer (FTIR) participated in functional group identification and chemical bonding of the samples, whereas UV–Visible spectrophotometry was responsible for evaluatingoptical properties. X-ray methods proved valuable in resolving the phase composition when results were to be settled or estimated. The synthesis process demanded a strict supply of high-purity chemicals that included the titanium precursor, titanium tetraisopropoxide (TTIP), solvent 2-propanol (alcohol), aniline for polymerization, potassium peroxydisulfate (PPD) as oxidant, and methanol. Distilled water was applied as a medium for reactions and washing procedures, while ortho nitroaniline orange served as a model contaminant for photocatalytic degradation studies. All chemicals and equipment were selected according to their reliability and compatibility with the experimental protocols, thus, ensuring that the whole research process was reproducible and accurate.

Experimental Procedure

Sample Preparation

The procedures for polyaniline (PANI) synthesis, titanium dioxide (TiO_2) nanoparticles, and PANI/TiO_2 nanocomposites were based on series of chemical methods that were strictly

controlled. The process of polymer synthesis of polyaniline was done by chemical oxidative polymerization through the use of aniline monomer, hydrochloric acid (HCl) as a dopant, and ammonium persulphate (APS) as an oxidizing agent. Over the course of 15 minutes polymerization APS was added to the aniline-HCl solution dropwise to obtain a PANI-HCl thin film. This entire procedure was conducted under different conditions of temperature (4 °C, 13 °C, and 31 °C) and HCl concentrations of 1 M and 2 M to form thin layers. These were then washed with distilled water and dried at room temperature. The TiO_2 nanoparticles were produced by the sol–gel method based on titanium tetraisopropoxide (TTIP), 2-propanol, and distilled water as the main reactants. To the 2-propanol, HCl was added until its pH reached 1.88, at which time TTIP was slowly added and the mixture was refluxed at 50 °C to create a sol. Finally, the sol was heated and distilled water was added thus the gel was aged, dried at 70 °C for 15 hours and finally calcinated at 500 °C to obtain TiO_2 nanopowder.

The PANI/TiO_2 nanocomposite was prepared by *in situ* oxidative polymerization involving dispersing 1 g of TiO_2 in 100 mL of 1 M HCl followed by adding 2 mL of polyaniline and 5 g of potassium peroxydisulfate, the latter being dissolved in 25 mL of distilled water. The mixing of the compounds was done by stirring for three hours at ambient temperature which led to a green precipitate that was filtered out, washed thoroughly first with distilled water, then with methanol, and dried. The wet precipitate was kept for 48 hours, then heated to 400 °C for one hour, cooled in the desiccator, and finally ground into a homogenous powder. Characterization of all samples was done through FTIR, XRD, UV–Visible spectroscopy, and DLS at room temperature. For studying the photocatalytic degradation, an ortho-nitroaniline orange dye stock solution was prepared by dissolving 1 g dye in distilled water, and adjusting the volume to 1,000 mL. Serial dilution to 10-50 ppm was performed to obtain the working concentrations. Additionally, HNO_3 and NaOH solutions were freshly prepared in order to assist the experimental processes, maintaining the consistency and repeatability in each synthesis step.

Experimental Design

Degradation experiments were performed by adding a fixed amount of nanocomposite (0.4 g) to a 250 mL conical flask containing 50 mL of a diluted solution of ortho nitroaniline orange dye. The flasks were sealed and placed in a photoreactor/shaker set to 150 rpm at 298 K for the required time period. After regular intervals, samples were withdrawn, and the final concentration of dye was measured at its maximum absorbance wavelength using a UV–Visible spectrophotometer equipped with a 1 cm quartz cell The amount of dye adsorbed at equilibrium (q_e, mg/g) was calculated using Equation (1):

$$q_e = \frac{(C_o - C_e)V}{W} \quad (1)$$

Where, C_o and C_e are the initial and equilibrium concentrations of the dye (mg/L), V is the volume of the solution (L), and W is the mass of adsorbent (g). Degradation efficiency was expressed by Equation (2):

$$\text{Degradation efficiency } (\%) = \frac{C_o - C_e}{C_o} \times 100 \quad (2)$$

The monitoring of pH influence on dye degradation occurred through the incremental adjustments with dilute HNO_3 or NaOH (0.1 M). Besides, temperature, contact time, and adsorbent dose were parameters that were varied as well to determine their influences on dye removal through the use of calibration curves for concentration determination.

Adsorption isotherms were assessed according to both the Langmuir and Freundlich models. The Langmuir isotherm in Equation (3) was applied in the assessment of maximum monolayer adsorption capacity, thereby:

$$\frac{C_e}{q_e} = \frac{1}{K_L q_m} + \frac{C_e}{q_m} \quad (3)$$

To validate the Langmuir model, a graph of C_e/q_e (y-axis) versus C_e (x-axis) was employed which also allowed the extraction of constant values from slope and intercept. Moreover, the dimensionless separation factor (K_L) was

computed to assess the adsorption direction. The Freundlich isotherm illustrated the variability in the adsorbent's surface characteristics, expressed in Equations (4) and (5) as:

$$q_e = K_f C_e^{1/n} \quad (4)$$

$$\log\ q_e = \log\ K_f + \frac{1}{n}\log\ C_e \quad (5)$$

Where, K_f and n are Freundlich constants that represent adsorption capacity and intensity, respectively.

Adsorption kinetics were analyzed through pseudo-first-order Equation (6) and pseudo-second-order Equation (7) models. The first-order kinetic equation is:

$$\log\ (q_e - q_t) = \log\ q_e - \frac{k_1}{2.303} t \quad (6)$$

Where, k_1 is the rate constant and q_t is the amount adsorbed at time t. The second-order model is expressed as:

$$\frac{t}{q_t} = \frac{1}{k_2 q_e^2} + \frac{t}{q_e} \quad (7)$$

With k_2 as the second-order rate constant, and initial sorption rate calculated accordingly.

Result and Discussion

The FTIR spectrum of TiO_2 nanoparticles (Figure 1) exhibits several characteristic absorption bands. The broad band observed at around 3,011 cm^{-1} is attributed to the stretching vibration of surface hydroxyl (–OH) groups, indicating the presence of adsorbed moisture. The band at approximately 1,640 cm^{-1} corresponds to the bending vibration of –OH groups of molecular water. The absorption band observed near 738 cm^{-1} is assigned to the Ti–O stretching vibration, which is a characteristic feature of TiO_2 nanoparticles [7].
A weak absorption band appearing around 946 cm^{-1} and a minor band near 2,117 cm^{-1} may be associated with surface-related species or trace impurities and do not indicate the formation of any secondary crystalline phase. These minor bands do not significantly affect the fundamental Ti–O framework of the synthesized TiO_2 nanoparticles.

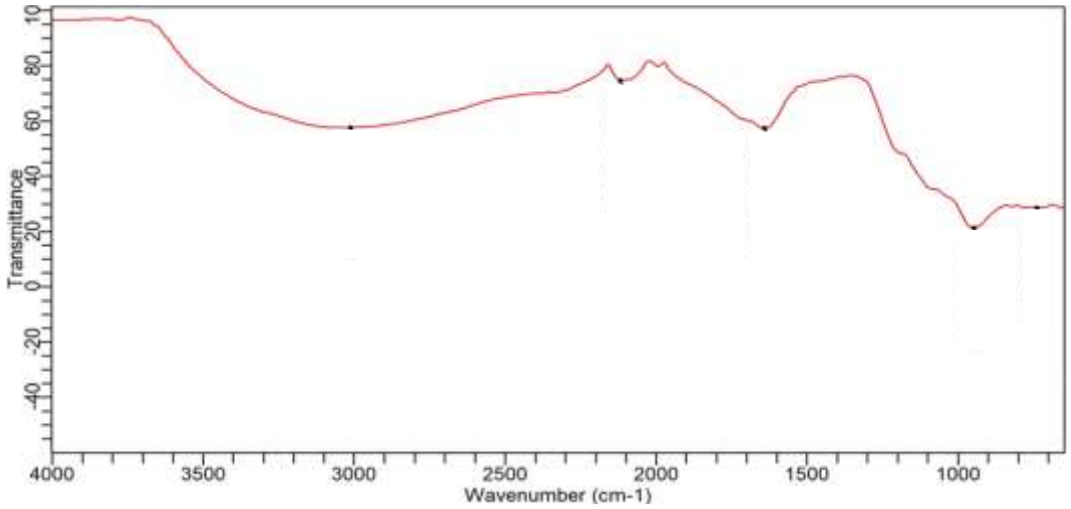

Figure 1. FTIR analysis of TiO_2

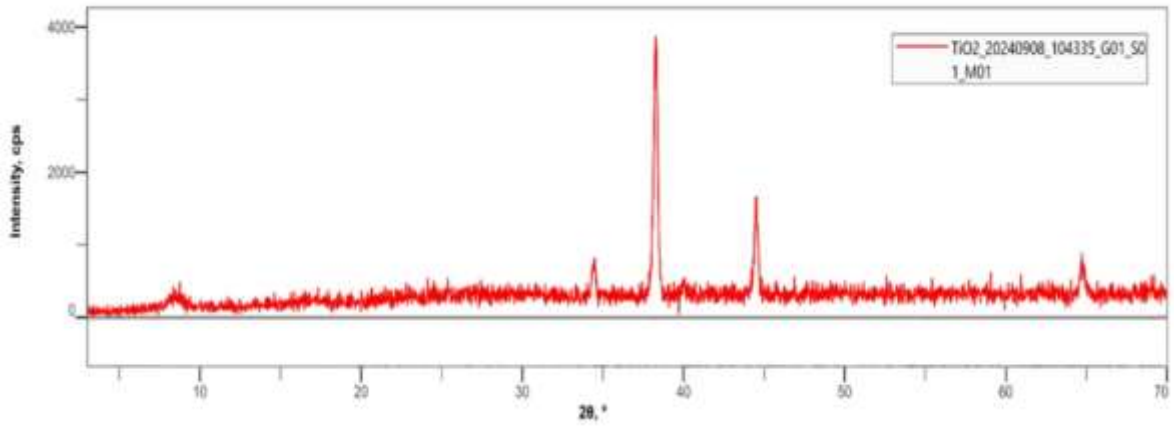

Figure 2. Peak of XRD spectra

Figure 2 represents the XRD pattern of the TiO_2 nanoparticle. Based on the XRD data, it is evident that TiO_2 nanoparticle exhibited different peaks at 2θ ≈ 27.4°, 36.1°, 41.2°, and 54.3° (rutile TiO_2, JCPDS No. 21-1276), which is relate to the rutile TiO_2. From the XRD pattern, it is evident that calcining at 500 °C results in rutile crystal phase transition [8].

The size was calculated using Debye-Scherre equation, $D = K\lambda/(\beta cos\theta)$ from this size was found to be 38.7 nm.

Where,

D: average crystallite size

K: shape factor 0.9

λ: wavelength of X-ray radiation

β: full width at half maximum (FWHM) of the diffraction peak

θ: Bragg angle

The optical properties of TiO_2 nanoparticles were investigated using UV–Visible spectroscopy, as shown in Figure 3. From the UV–Visible absorption analysis, the optical band gap of the synthesized TiO_2 nanoparticles was estimated to be approximately 3.0 eV using the Tauc method. The band gap energy was calculated using Equation (8). The dotted lines represent the absorption properties of TiO_2.

$$(\alpha h\nu)^2 = A(h\nu - Eg) \quad (8)$$

Where, α represents the absorption coefficient, hν denotes the photon energy, Eg is the optical band gap energy, and A is a material-dependent constant.

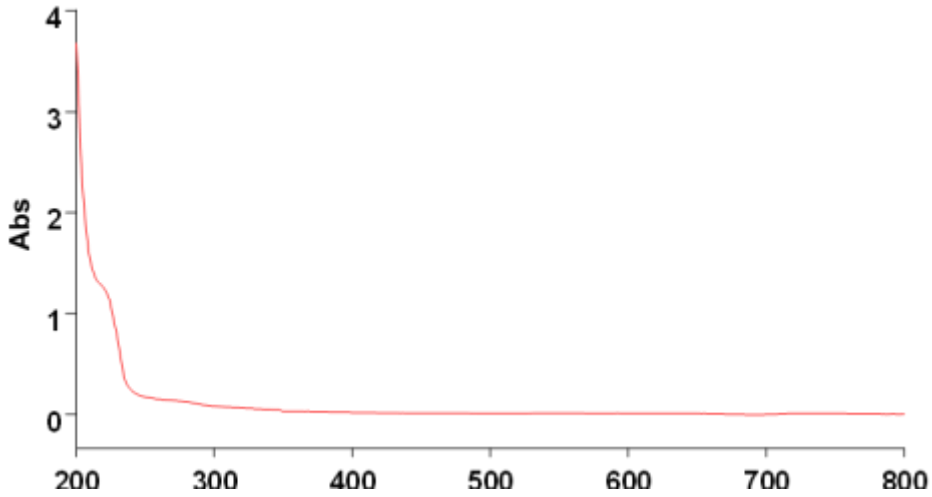

Figure 3. UV-Visible absorption analysis of TiO_2

Conclusion

X-ray diffraction (XRD) analysis provided clear evidence of the successful synthesis of TiO_2 nanoparticles predominantly in the rutile phase, as indicated by the sharp diffraction peaks. The phase transformation from anatase to rutile was mainly attributed to the calcination temperature of 500 °C, which is consistent with reported studies indicating that anatase-to-rutile transformation occurs between 500 and 600 °C. The average crystallite size of the synthesized TiO_2 nanoparticles was estimated to be 38.7 nm using the Debye–Scherrer equation, indicating good crystallinity. UV–Visible spectroscopic analysis revealed that the synthesized TiO_2 nanoparticles exhibit an optical band gap of approximately 3.0 eV, which aligns with reported values for rutile TiO_2 and supports their photocatalytic performance under UV irradiation. The obtained rutile-phase TiO_2 nanoparticles demonstrate promising potential for the photocatalytic degradation of organic dyes due to their improved charge transfer characteristics and reduced electron–hole recombination. In addition, these nanoparticles can be employed in water splitting, antibacterial, antioxidant, and dye-sensitized solar cell applications, with photocatalytic efficiencies comparable to those of the anatase phase.

Conflict of Interest

No conflicts of interest were reported by the authors in this work.

ORCID

Shamsuddeen Musa
https://orcid.org/0009-0006-6223-105X
Dahiru Adamu Ajiya
https://orcid.org/0000-0002-0628-7757
Samuel Adebayo Adeyanju
https://orcid.org/0009-0006-1042-5100

Reference

[1] Singh, N., Rai, S., Agarwal, S. Polymer nanocomposites and Cr (VI) removal from water. *Nanosci. Technol*, **2014**, 1, 1-10.

[2] Soylemez, S., Hacioglu, S.O., Kesik, M., Unay, H., Cirpan, A., Toppare, L. A novel and effective surface design: conducting polymer/β-cyclodextrin host–guest system for cholesterol biosensor. *ACS Applied Materials & Interfaces*, **2014**, 6(20), 18290-18300.

[3] Raymond, J.E., Vohs, J.K., Brege, J.J., Rozeveld, S., LeCaptain, D.J., Slusher, L.E., Fahlman, B.D. Room-Temperature Growth of Carbon Nanofibers from Iron-Encapsulated Dendritic Catalysts. *Polymer News*, **2005**, 30(10), 330-333.

[4] Khalid, N., Abd Razak, J., Hasib, H., Ismail, M., Mohamad, N., Junid, R., Puspitasari, P. A short review on polyaniline (PANI) based nanocomposites for various applications: enhancing the electrical conductivity. In *IOP Conference Series: Materials Science and Engineering*, **2020**, 957, 12028.

[5] Nicolas-Debarnot, D., Poncin-Epaillard, F. Polyaniline as a new sensitive layer for gas sensors. *Analytica Chimica Acta*, **2003**, 475(1-2), 1-15.

[6] Padmini, R., Nallal, V.U.M., Razia, M., Sivaramakrishnan, S., Alodaini, H.A., Hatamleh, A.A., Chung, W.J. Cytotoxic effect of silver nanoparticles synthesized from ethanolic extract of Allium sativum on A549 lung cancer cell line. *Journal of King Saud University-Science*, **2022**, 34(4), 102001.

[7] Wei, Y., Jang, G.W., Hsueh, K.F., Scherr, E.M., MacDiarmid, A.G., Epstein, A.J. Thermal transitions and mechanical properties of films of chemically prepared polyaniline. *Polymer*, **1992**, 33(2), 314-322.

[8] Alheety, M.A., Majeed, A.H., Ali, A.H., Mohammed, L.A., Destagul, A., Singh, P.K. Synthesis and characterization of eggshell membrane polymer-TiO_2 nanocomposite for newly synthesized ionic liquid release. *Journal of the Iranian Chemical Society,* **2022**, 19(9), 4005-4015.

[9] Senevirathne, K., Burns, A.W., Bussell, M.E., Brock, S.L. Synthesis and characterization of discrete nickel phosphide nanoparticles: effect of surface ligation chemistry on catalytic hydrodesulfurization of thiophene. *Advanced Functional Materials*, **2007**, 17(18), 3933-3939.

[10] Gupta, S.M., Tripathi, M. A review of TiO_2 nanoparticles. *Chinese Science Bulletin*, **2011**, 56, 1639–1657.

[11] Nabi, G., Khalid, N., Tahir, M.B., Rafique, M., Rizwan, M., Hussain, S., Majid, A. A review on novel eco-friendly green approach to synthesis TiO_2 nanoparticles using different extracts. *Journal of Inorganic and Organometallic Polymers and Materials*, **2018**, 28(4), 1552-1564.

[12] Zietal, D., Czarczynska-Goslinska, B., Mlynarczyk, D.T., Glowacka-Sobotta, A., Stanisz, B., Goslinski, T., Sobotta, L. Titanium dioxide

nanoparticles: prospects and applications in medicine. *Nanomaterials*, **2020**, 10(2), 387.
[13] Piccinno, F., Gottschalk, F., Seeger, S., Nowack, B. Industrial production quantities and uses of ten engineered nanomaterials in Europe and the world. *Journal of Nanoparticle Research*, **2012**, 14(9), 1109.
[14] Nabi, G., Raza, W., Tahir, M. Green synthesis of TiO_2 nanoparticle using cinnamon powder extract and the study of optical properties. *Journal of Inorganic and Organometallic Polymers and Materials*, **2020**, 30(4), 1425-1429.
[15] Hayle, S.T. Synthesis and characterization of titanium oxide nanomaterials using sol-gel method. *American Journal of Nanoscience and Nanotechnology*, **2014**, 2, 1–7.
[16] Chen, X.F., Xu, Y., Liu, W., Ding, H., Hou, X. F., Wan, Y., Wang, Y., Ji, J.F. Study on the properties of composite titanium dioxide and its application in decorative base paper. *Transactions of China Pulp and Paper*, 2015, 34, 1–6.
[17] Ismael, M. Highly effective ruthenium-doped TiO_2 nanoparticles photocatalyst for visible-light-driven photocatalytic hydrogen production. *New Journal of Chemistry*, **2019**, 43(24), 9596-9605.
[18] Ananthanarayanan, D., Leon, J.J.D., Wong, J., Nicolay, S., Aberle, A.G., Ho, J.W. Mid-infrared characterization and modelling of transparent conductive oxides. *Solar Energy*, **2020**, 209(424-430.
[19] Ismael, M. Latest progress on the key operating parameters affecting the photocatalytic activity of TiO_2-based photocatalysts for hydrogen fuel production: A comprehensive review. *Fuel*, **2021**, 303, 121207.
[20] Van Chuong, T., Khieu, D.Q. Synthesis of nano titanium dioxide and its application in photocatalysis. *Journal of the Korean Physical Society*, **2008**, 1526-1529.
[21] Duarte, A., Amorim, M.T.P. Photocatalytic treatment techniques using titanium dioxide nanoparticles for antibiotic removal from water. *Application of Titanium Dioxide*, **2017**, 125-146.
[22] Marimuthu, S., Rahuman, A.A., Jayaseelan, C., Kirthi, A.V., Santhoshkumar, T., Velayutham, K., Iyappan, M. Acaricidal activity of synthesized titanium dioxide nanoparticles using Calotropis gigantea against Rhipicephalus microplus and Haemaphysalis bispinosa. *Asian Pacific Journal of Tropical Medicine*, **2013**, 6(9), 682-688.
[23] Aslam, M., Abdullah, A.Z., Rafatullah, M. Recent development in the green synthesis of titanium dioxide nanoparticles using plant-based biomolecules for environmental and antimicrobial applications. *Journal of Industrial and Engineering Chemistry*, **2021**, 98, 1-16.
[24] Goutam, S.P., Saxena, G., Singh, V., Yadav, A.K., Bharagava, R.N., Thapa, K.B. Green synthesis of TiO_2 nanoparticles using leaf extract of Jatropha curcas L. for photocatalytic degradation of tannery wastewater. *Chemical Engineering Journal*, **2018**, 336, 386-396.
[25] Lazar, M.A., Varghese, S., Nair, S.S. Photocatalytic water treatment by titanium dioxide: recent updates. *Catalysts*, **2012**, 2(4), 572-601.
[26] Kaur, G., Kaur, H., Kumar, S., Verma, V., Jhinjer, H.S., Singh, J., Al-Rashed, S. Blooming approach: one-pot biogenic synthesis of TiO_2 nanoparticles using piper betle for the degradation of industrial reactive yellow 86 Dye. *Journal of Inorganic and Organometallic Polymers and Materials*, **2021**, 31(3), 1111-1119.
[27] Khade, G., Suwarnkar, M., Gavade, N., Garadkar, K. Green synthesis of TiO_2 and its photocatalytic activity. *Journal of Materials Science: Materials in Electronics*, **2015**, 26(5), 3309-3315.